J. Fluid Mech. (1971), *vol.* 50, *part* 4, *pp.* 785–799
Printed in Great Britain

A numerical investigation into the effects of compressibility and total enthalpy difference on the development of a laminar free shear layer

By PETER W. CARPENTER
Department of the Mechanics of Fluids, University of Manchester

(Received 14 March 1971)

A method is presented for integrating numerically the equations of motion for a compressible free shear layer developing from a boundary-layer profile of arbitrary shape. Sutherland's law is used to determine the coefficient of viscosity and the Prandtl number is taken as 0·72. Calculated results are reported for free-stream Mach numbers ranging from 0 to 10 and for stagnation–enthalpy ratios ranging from 0 to 5·0. The effects of varying the initial boundary-layer profile and of a discontinuity in temperature at the origin are also studied. The results include graphs showing the development of dividing-streamline velocity, of local Nusselt number, and of dividing-streamline location.

1. Occurrence of free shear layers in nature

When free shear layers exist as separate entities, as for instance in the atmosphere or ocean, they are usually considered to be fully developed for all practical purposes. In addition, they are almost always either turbulent or mixing layers forming at the interface of two different fluids. Thus, generally speaking, the development of a laminar free shear layer from some sort of boundary-layer profile is only important when the shear layer is a component of a more complicated flow field. The flow about a bluff body provides a good example. To see how free shear layers are formed under these circumstances it is necessary to study the flow patterns corresponding to the limit $Re \to \infty$. Owing to the presence of certain singular surfaces, known as free streamlines, these patterns are fundamentally different from the potential-flow ($Re = \infty$) ones.† The presence of a free shear layer is required by nature to smooth out the infinite velocity gradient at the singular surface.

Owing to their instability these limiting flow patterns rarely occur at subsonic speeds and are largely of academic interest only. On the other hand, the hyperbolic character of the inviscid flow field in the supersonic regime has a stabilizing influence, and the corresponding limiting flow patterns should be of considerable practical importance for the solution of many separated-flow problems. The rearward- and forward-facing steps, blunt-based bodies and rectangular cavities are typical examples. Indeed, a well-known method of approach due to Chapman

† These patterns are discussed by Batchelor (1956).

(1950) and Korst (1956) assumes that the processes in the free shear layer dominate the entire flow field in such phenomena.

In reality it seems probable that the shear layer usually develops between a subsonic vortical region and a supersonic stream. However, this paper deals with the simpler problem where the vortical region is replaced by a quiescent one. This is considered to be a necessary prelude to the solution of the more difficult problem. In addition it might be noted that the Chapman–Korst model theories also usually assume a 'dead-air' region.

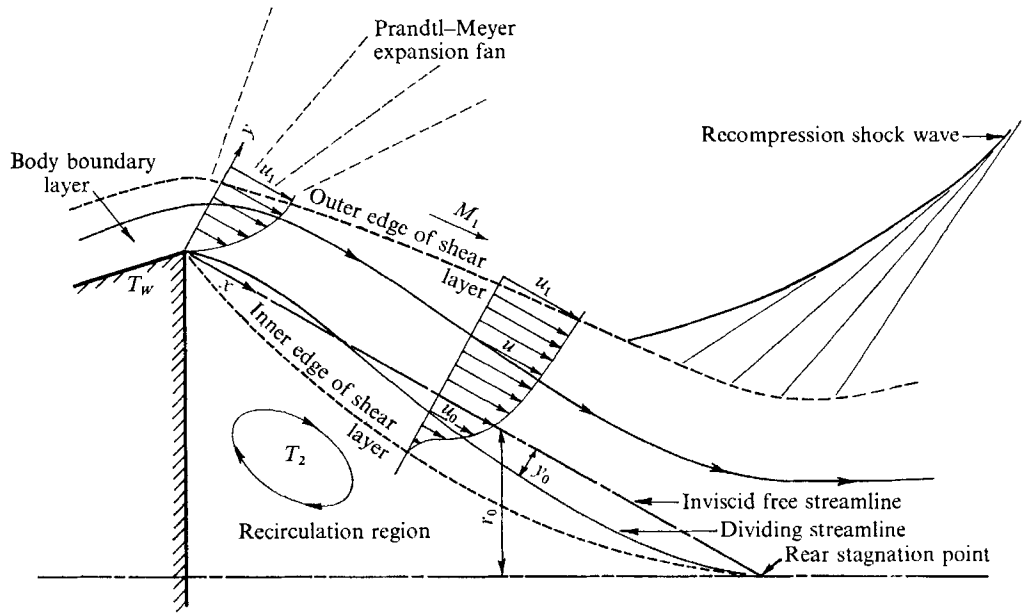

FIGURE 1. The free shear layer as a component of the flow field behind a blunt-based body travelling at a supersonic speed.

Figure 1 shows the free shear layer as a component in the flow field behind a blunt-based body travelling at a supersonic speed. This provides an example of a separated-flow phenomenon where the properties of a developing free shear layer are of paramount importance. In order to carry out engineering calculations on such flows it is necessary to know the values of such parameters as the heat-transfer coefficient and velocity at the dividing streamline. (The dividing streamline separates the air once in the body boundary layer from that entrained from the recirculation region.) For the purposes of calculation it is commonly assumed that these parameters have their fully developed self-similar values along the length of the dividing streamline.

One of the objects of this paper is to examine the accuracy of this assumption when the free-stream Mach number M_1 and temperature (or total enthalpy) T_2 (or H_2) in the recirculation region are varied, given a particular initial boundary-layer momentum thickness δ_0^{**}. Since there can be considerable heat transfer both through the base wall and from the body boundary layer, it is quite possible for the temperature T_W at the surface of the body boundary layer just before

separation to be considerably different from that in the recirculation region. Therefore the effects of this situation on the shear-layer development are examined. Finally, the influence of the actual shape of the body boundary-layer velocity profile is examined, although the effect of the Prandtl–Meyer expansion is not considered explicitly.

2. Discussion of problem and its main difficulties

After making the boundary-layer approximation and assuming constant pressure, the continuity, momentum and energy (in total enthalpy formulation) equations may be written as follows.

$$\frac{\partial}{\partial x}(\rho u r_0^\nu) + \frac{\partial}{\partial y}(\rho v r_0^\nu) = 0, \tag{2.1}$$

$$\rho u \frac{\partial u}{\partial x} + \rho v \frac{\partial u}{\partial y} = \frac{\partial}{\partial y}\left(\mu \frac{\partial u}{\partial y}\right), \tag{2.2}$$

$$\rho u \frac{\partial H}{\partial x} + \rho v \frac{\partial H}{\partial y} = \frac{\partial}{\partial y}\left[\frac{\mu}{\sigma}\frac{\partial}{\partial y}\left\{H + (\sigma - 1)\frac{u^2}{2}\right\}\right], \tag{2.3}$$

where
$$\nu = \begin{cases} 0, & \text{plane shear layer} \\ 1, & \text{axisymmetric.} \end{cases}$$

r_0 is the distance of the free streamline, or inviscid jet surface, from the axis of symmetry; $H = C_p T + \frac{1}{2}u^2$, the total enthalpy; $\sigma = C_p \mu / k$, the Prandtl number.

The objective is to obtain an accurate numerical solution to (2.1), (2.2) and (2.3) subject to the boundary conditions given below.

$$\left.\begin{aligned} &u \to u_1, \quad H \to H_1 \quad \text{as} \quad y \to +\infty, \\ &u \to 0, \quad H \to H_2 \quad \text{as} \quad y \to -\infty, \\ &v = 0 \quad \text{at} \quad y = y_0(x) \end{aligned}\right\} \tag{2.4}$$

and
$$u(0, y) = u_i(y), \quad H(0, y) = H_i(y), \tag{2.5}$$

where y_0 is the position of the dividing streamline, so-called because it is the interface between air once in the boundary layer and that entrained from the quiescent region.

The method of integration is to be applicable for any initial boundary-layer profiles, i.e. arbitrary $u_i(y)$ and $H_i(y)$, and for any value of H_2/H_1. Quite apart from the obviously difficult task of integrating numerically a complicated system of second-order non-linear partial differential equations over an infinite domain, the problem of the free shear layer possesses two special difficulties. These make it more interesting in some ways than the corresponding attached boundary layer. The two difficulties referred to are as follows.

(i) *Apparent non-uniqueness of the solution.* Note that the position of the

dividing streamline, $y_0(x)$, in (2.4) is unknown *a priori*. However the equations may be solved in the xu plane, leaving the orientation in space arbitrary. Ting (1959) has shown that in order to fix $y_0(x)$ it is necessary to investigate the higher order corrections to the boundary-layer solution. This is in sharp contrast to the attached boundary layer where the zeroth-order solution can be determined uniquely, independently of the higher order corrections.

(ii) *Singularity at the origin.* This singularity has two aspects. First, as pointed out by Goldstein (1930), if the initial velocity profile is specified arbitrarily, without regard for the pressure distribution, then, in general, the existence of an algebraic singularity at the origin seriously hampers any attempt to continue integration downstream. To understand this note that at $(0, 0)$ $u = 0$ and $v = 0$ but in general $\partial(\mu\,\partial u/\partial y)/\partial y \neq 0$, therefore in order to satisfy the momentum equation (2.2) $\partial u/\partial x$ must be $O(u^{-1})$ as $y \to +0$ at $x = 0$. Of course, strictly speaking this shows that near the origin the boundary-layer equations are no longer valid. However this is ignored, the justification being the small extent of the region of invalidity. Second, a discontinuity in the boundary conditions arises at the origin, since at $x = 0$, $u = 0$ and $H = H_W$ $(T = T_W)$ at $y = 0$; whereas under the limit $x \to +0$, $u \to 0$ and $H \to H_2$ $(T \to T_2)$ as $y \to -\infty$.

To date no solution for the developing free shear layer successfully overcoming both these difficulties appears to have been published. However, Denison & Baum (1963) have obtained results corresponding to a Blasius profile as initial condition. They used a local expansion, suggested by Goldstein (1930), to tackle the singularity at the origin. The problem of determining y_0 was left unsolved.

3. Analysis

The choice of the method of numerical integration was dictated to a large extent by the difficulties discussed in the foregoing section. Because of these it is desirable to carry out the integration in Crocco co-ordinates. The use of these co-ordinates has three main advantages: (i) The solution is independent of $y_0(x)$ in the xu plane, allowing $y_0(x)$ to be determined *a posteriori*. (ii) It removes the difficulty of the discontinuity in the velocity boundary condition. (iii) The domain will be bounded.

Concomitant with these assets, however, is a difficulty in the shape of troublesome singularities at $u = 0$ and $u = u_1$. A modification of the Dorodnitsyn (1962) method of integral relations was considered to provide the best means of dealing with these singularities and the remaining problems at the origin. This method also has advantages for avoiding numerical instabilities.

Essentially, when this technique is employed, the solution is carried out in two main stages. First, the system of partial differential equations is reduced to one of first-order ordinary differential equations. Then this system is integrated numerically using some suitable technique.

The initial stage in the reduction is the derivation of two sets of integral relations. Suppose there exist two sets of weighting functions $f_j(u)$ and $g_k(H)$ which are linearly independent and piecewise continuous in u. (Additional requirements will be imposed later.) Now mutliply (2.1) by $f_j(u)$ and (2.2) by $r_0^\nu df_j/du$

and integrate their sum with respect to y from $-\infty$ to $+\infty$. Thereby the following system of equations is obtained.

$$\frac{d}{dx}\int_{-\infty}^{\infty}\rho u r_0^{\nu} f_j(u)\,dy + [\rho v r_0^{\nu} f_j(u)]_{-\infty}^{\infty} = \int_{-\infty}^{\infty}\frac{\partial}{\partial y}\left(r_0^{\nu}\mu\frac{\partial u}{\partial y}\right) f_j'(u)\,dy. \tag{3.1}$$

Now in order to eliminate v from (3.1) it is required that

$$f_j(u_1) = f_j(0) = 0. \tag{3.2}$$

Integration of the right-hand side by parts leads to the following set of integral relations.

$$\frac{d}{dx}\int_{-\infty}^{\infty}\rho u r_0^{\nu} f_j(u)\,dy = -\int_{-\infty}^{\infty}\mu r_0^{\nu}\left(\frac{\partial u}{\partial y}\right)^2 f_j''(u)\,dy \quad (j = 0, 1, 2, \ldots). \tag{3.3}$$

A similar operation with (2.3) and the $g_k(H)$ results in a second set of integral relations, viz.

$$\frac{d}{dx}\int_{-\infty}^{\infty}\rho u r_0^{\nu} g_k(H)\,dy = -\int_{-\infty}^{\infty}\frac{\mu}{\sigma}\frac{\partial}{\partial y}[H + (\sigma - 1)\tfrac{1}{2}u^2]\, g_k''(H)\, r_0^{\nu}\,dy, \tag{3.4}$$

where $k = 0, 1, 2, \ldots$, and the requirement

$$g_k(H_1) = g_k(H_2) = 0 \tag{3.5}$$

has been imposed.

Now the reduction of equations (3.3) and (3.4) to a system of first-order ordinary differential equations is effected. The integral relations (3.3) and (3.4) are non-dimensionalized, using the following definitions:

$$\bar{x} = x/L, \quad \bar{y} = y/L, \quad \bar{u} = u/u_1,$$
$$\bar{H} = H/H_1, \quad \bar{\rho} = \rho/\rho_1, \quad \bar{\mu} = \mu/\mu_1,$$

L being some characteristic length (e.g. the boundary-layer momentum thickness at the origin, δ_0^{**}). Next the transformation

$$\xi = \frac{L u_1 \rho_1}{\mu_1}\int r_0^{2\nu}\,d\bar{x}; \quad \eta = \int \bar{\rho} r_0^{\nu}\,d\bar{y} \tag{3.6}$$

is applied. This is done because ultimately it is necessary to integrate the left-hand sides of the integral relations analytically. In addition, the relations are now independent of r_0 and Reynolds number. Finally, the integral relations are cast into Crocco co-ordinates, producing

$$\frac{d}{d\xi}\int_0^1 \bar{u} f_j(\bar{u})\,\zeta(\xi, \bar{u})\,d\bar{u} = -\int_0^1 \bar{\mu}\bar{\rho} f_j''(\bar{u})\frac{1}{\zeta}\,d\bar{u} \quad (j = 0, 1, 2, \ldots), \tag{3.7}$$

and

$$\frac{d}{d\xi}\int_0^1 \bar{u} g_k(\bar{H})\,\zeta(\xi, \bar{u})\,d\bar{u} = \frac{1}{\sigma}\left\{\int_0^1 \bar{\rho}\bar{\mu}\left(\frac{\partial \bar{H}}{\partial \bar{u}}\right)^2 g_k''\frac{1}{\zeta}\,d\bar{u} + \frac{2(\sigma - 1)(\gamma - 1)M_1^2}{2 + (\gamma - 1)M_1^2}\int_0^1 \bar{\rho}\bar{\mu}\bar{u}\frac{\partial \bar{H}}{\partial \bar{u}} g_k''\frac{1}{\zeta}\,d\bar{u}\right\} \quad (k = 0, 1, 2, \ldots), \tag{3.8}$$

where $\zeta(\xi, \bar{u}) = \partial\eta/\partial\bar{u}$.

Partly because of the difficulty with the boundary-condition discontinuity at the origin and partly owing to the asymptotic behaviour of $\zeta(\xi, \bar{u})$ and $\bar{H}(\xi, \bar{u})$

at $\bar{u} = 1$ and 0, it is virtually a necessity to divide the domain into two strips. The dividing streamline provides a logical choice of interface.†

Designating quantities in the upper and lower strips by superscripts u and l respectively, the following choices of weighting functions are made.

$$\left.\begin{aligned} f_j^l(\bar{u}) &= \bar{u}^{j+1} \quad (\bar{u} < \bar{u}_0), \\ f_j^u(\bar{u}) &= \bar{u}^{j+1} - 1 \quad (\bar{u} > \bar{u}_0), \end{aligned}\right\} \quad (j = 0, 1, 2, \ldots), \tag{3.9}$$

$$\left.\begin{aligned} g_k^l(\bar{H}) &= \bar{H}^{k+1} - \lambda^{k+1} \quad (\bar{u} < \bar{u}_0), \\ g_k^u(\bar{H}) &= \bar{H}^{k+1} - 1 \quad (\bar{u} > \bar{u}_0), \end{aligned}\right\} \quad (k = 0, 1, 2, \ldots), \tag{3.10}$$

where $\lambda = H_2/H_1$.

The dependent variables $\zeta(\xi, \bar{u})$ and $\bar{H}(\xi, \bar{u})$ are approximated by the following expressions.

$$\left.\begin{aligned} \zeta^l(\xi, \bar{u}) &= \frac{1}{\bar{u}} \sum_{m=1}^{M} b_m(\xi)\, \bar{u}^{m-1} \quad (\bar{u} < \bar{u}_0), \\ \zeta^u(\xi, \bar{u}) &= \frac{1}{1-\bar{u}} \sum_{m=1}^{M} a_m(\xi)\, (1-\bar{u})^{m-1} \quad (\bar{u} > \bar{u}_0), \end{aligned}\right\} \tag{3.11}$$

and

$$\left.\begin{aligned} \bar{H}^l(\xi, \bar{u}) &= \{\lambda + (1-\lambda)\,\bar{u}\} \sum_{n=1}^{N} d_n(\xi)\, \bar{u}^{n-1} \quad (\bar{u} < \bar{u}_0), \\ \bar{H}^u(\xi, \bar{u}) &= \{\lambda + (1-\lambda)\,\bar{u}\} \sum_{n=1}^{N} c_n(\xi)\, (1-\bar{u})^{n-1} \quad (\bar{u} > \bar{u}_0). \end{aligned}\right\} \tag{3.12}$$

Approximating ζ in this way takes care of the singularity at $\bar{u} = 0$ and 1. The functions of $\bar{u}$ premultiplying the polynomials in (3.11) and (3.12) were determined by an asymptotic analysis of (2.1), (2.2) and (2.3) in Carpenter (1970). The coefficients b_m can be obtained in terms of a_m and $\bar{u}_0$ by requiring continuity of ζ and its derivatives of all orders up to $M-1$, at the dividing streamline. Similarly the d_n are found in terms of the c_n by requiring continuity of $\bar{H}$ and its derivatives.

If the above expressions and approximations are substituted into (3.7) and (3.8) and the left-hand side integrals evaluated analytically, the result is a system of first-order non-linear ordinary differential equations. The dependent variables are $\bar{u}_0; a_1, \ldots, a_M; c_1, \ldots, c_N$. $M+1$ of the equations are furnished by equations (3.7), with the remaining N coming from equations (3.8). The system can be represented succinctly by using a matrix formulation

$$A_{ij}\, dB_j/d\xi = C_i \quad (1 \leqslant i, j \leqslant 1 + M + N), \tag{3.13}$$

where repeated indices are summed, A_{ij} and C_i depend on ξ and the dependent variables B_j. The C_i are found by integrating the right-hand sides of (3.7) and (3.8) numerically.

As things stand the matrix A_{ij} is singular at $\xi = 0$. This is because of the algebraic singularity at the origin which results in $d\bar{u}_0/d\xi \to \infty$ as $\xi \to +0$. This difficulty is overcome by replacing $\bar{u}_0$ with $\frac{1}{2}\bar{u}_0^2$ as dependent variable. (The physical significance of this parameter will be discussed in the next section.)

† Since $v = 0$ at $y = y_0$ this choice obviates any additional restrictions on the weighting functions for preserving the validity of (3.3).

Clearly the boundedness of $d(\frac{1}{2}\bar{u}_0^2)/d\xi = \bar{u}_0 d\bar{u}_0/d\xi$ follows directly from the momentum equation. The discontinuity in the boundary condition on $\bar{H}$ is handled by setting $c_1(0) = H_w/H_2 = \lambda_w$.

It can be shown that if the number M of the coefficients $a_m(\xi)$ in equation (3.11) is even, then it is impossible to simultaneously satisfy both the condition that a_1 and b_1 be positive and that

$$\left.\frac{\partial^{M-1}\zeta^u}{\partial\bar{u}^{M-1}}\right|_{\bar{u}=\bar{u}_0} = \left.\frac{\partial^{M-1}\zeta^l}{\partial\bar{u}^{M-1}}\right|_{\bar{u}=\bar{u}_0}.$$

Therefore only odd integral orders of approximating polynomials are admissible in (3.11).

The location of the dividing streamline must now be determined. The requirement that the normal stress be continuous has been used by Lock (1951) to fix y_0 for the heterogeneous free shear layer. But in the homogeneous case he found that the continuity condition was automatically satisfied. Therefore he concluded that in this instance the position of the interface was indeterminate. However, this automatic satisfaction ceases to occur when the higher order correction terms to the boundary-layer solution are considered. This allows Lock's principle to be extended to compressible homogeneous mixing.

The extended principle may be stated as follows. The 'displacement' effects of the shear layer on the main and secondary streams produce a higher order correction to the predicted flow field. The dividing streamline must be oriented such that this correction maintains a continuous normal stress across the entire shear layer.

This principle was introduced by Ting (1959) who applied it by carrying out an asymptotic analysis of the Navier–Stokes equations. He found that the principle leads to the condition

$$v(x, +\infty) = 0 \tag{3.14}$$

for the shear-layer solution. Carpenter (1970) has shown that this may be rewritten in the form

$$\frac{d\bar{y}_0}{d\xi} + \frac{1}{\bar{r}_0^{\nu}(1-\bar{\rho}_0\bar{u}_0)}\frac{d\delta_1}{d\xi} = 0, \tag{3.15}$$

where

$$\delta_1 = \int_{\bar{y}_0}^{\infty}(1-\bar{\rho}\bar{u})\,d\bar{y}.$$

It also transpires that Ting's simple matching procedure breaks down in the general case of a free shear layer developing along a curved free streamline. Consequently (3.15) would no longer be applicable. Nevertheless, Carpenter (1970) has shown that it still remains a reasonable approximation in some cases. Equation (3.15) is, in effect, a first-order ordinary differential equation for $\bar{y}_0$ and can be integrated step by step as the main integration proceeds downstream.

4. Discussion of results

Extensive numerical calculations were performed for air at a free-stream stagnation temperature of 275 °K. The approximations of $\zeta(\xi, \bar{u})$ and $\bar{H}(\xi, \bar{u})$ were made using six parameters, namely a_1, a_2, a_3, c_1, c_2 and $\frac{1}{2}\bar{u}_0^2$ (i.e. $M = 3, N = 2$).

Consequently it was necessary to integrate a system of six first-order ordinary differential equations. This was accomplished by marching downstream, using the simple trapezoidal rule with a matrix inversion. The step size was determined by requiring a specific increment in one of the dependent variables, usually $\frac{1}{2}\bar{u}_0^2$. The integration was normally continued until asymptotic fully developed conditions were attained for all practical purposes.

Sutherland's law was used for the coefficient of viscosity. The Prandtl number was set at 0·72. The coefficient of thermal conductivity was assumed to vary as $T^{0.85}$ (Brown & Donoughe 1951). The free-stream static temperature was taken to correspond to an isentropic expansion from $M = 0$ to M_1. The Blasius profile in $\bar{u}, \eta$ co-ordinates was taken as the initial condition, except for figure 9.

Probably, the development of free shear layers can best be understood physically in terms of a vorticity transfer.† Since vorticity cannot be created in the interior of the fluid, the vorticity flux† per unit time through a cross-section of

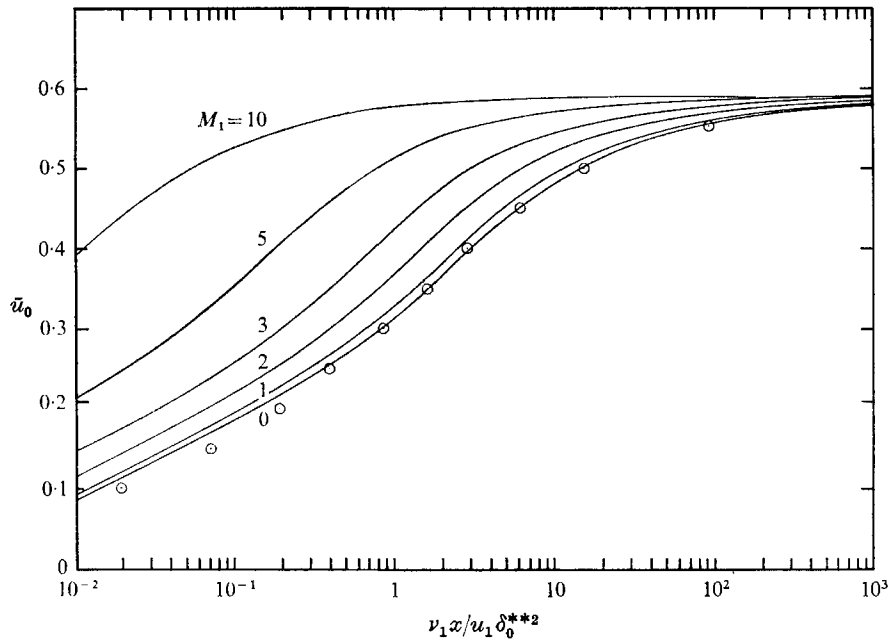

FIGURE 2. The effect of compressibility on the development of velocity at the dividing streamline with the Blasius profile in $\bar{u}$, η co-ordinates used as an initial condition. $H_2/H_1 = H_W/H_1 = 1{\cdot}0$; $Pr = 0{\cdot}72$; free-stream stagnation temperature = 275 °K; ⊙, Denison & Baum (1963).

the free shear layer remains constant. Thus if the boundary-layer approximation is used, the proportion of the vorticity flux below the dividing streamline is given by

$$-\int_{-\infty}^{\bar{y}_0} \bar{u}\frac{\partial \bar{u}}{\partial \bar{y}}\,d\bar{y} = -\frac{1}{2}\int_{-\infty}^{\bar{y}_0} \frac{\partial \bar{u}^2}{\partial \bar{y}}\,d\bar{y} = -\tfrac{1}{2}\bar{u}_0^2.$$

† Following common usage the word 'vorticity' is used rather loosely here. Strictly, one means 'circulation transfer' and 'circulation flux'.

Thereby the physical significance of this parameter, which was used in the analysis, is made clear.

At the origin a discontinuity in the vorticity profile exists and consequently vorticity diffuses to the lower stream to smooth out the infinite gradient. As the diffusion continues, the driving gradient is decreased by the smoothing-out process and the level of vorticity at the dividing streamline rises. Eventually, sufficient vorticity is transferred for it to reach a maximum at the dividing streamline and the diffusion across it ceases so that the asymptotic condition is achieved.

One would surmise that since the effect of compressibility is to intensify the diffusion process, then the development of a free shear layer to asymptotic conditions would be more rapid the higher the Mach number. Examination of figure 2 shows this to be, in fact, true.

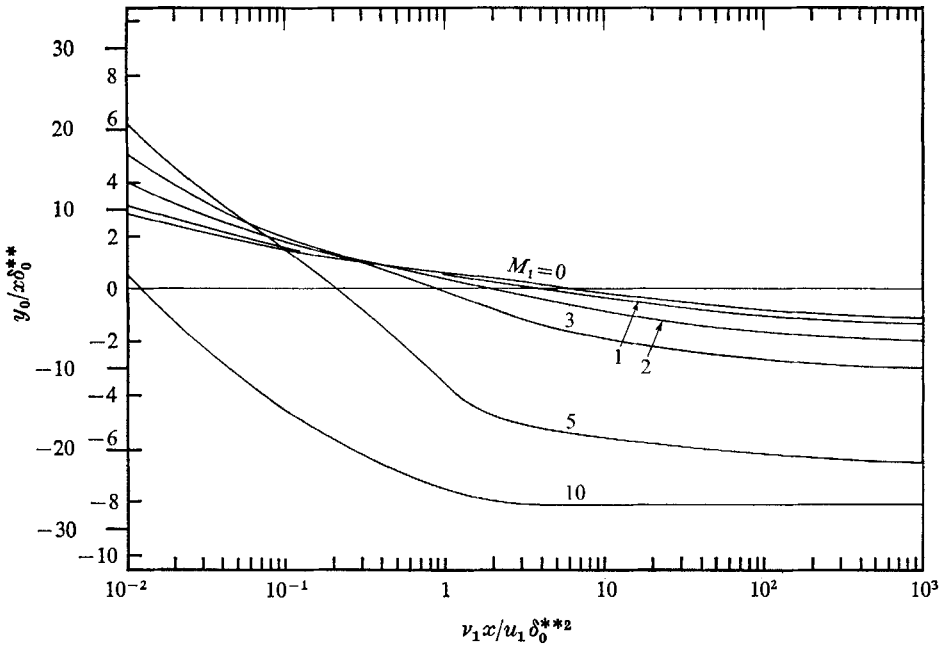

FIGURE 3. The effect of compressibility on the position of the dividing streamline with the Blasius profile in $\bar{u}$, η co-ordinates used as an initial condition. $H_2/H_1 = H_W/H_1 = 1{\cdot}0$; $Pr = 0{\cdot}72$; free-stream stagnation temperature = 275 °K; the wider scale corresponds to case of $M_1 = 10$.

It is a rather singular feature of the free shear layer that the asymptotic value of $\bar{u}_0$ does not alter significantly with M_1. That is to say, the lower stream's share of the total vorticity flux is virtually unaffected by compressibility. No explanation is presented here, although it might be noted that the vorticity transferred relative to the x axis does increase with M_1 since at higher Mach numbers the dividing streamline is deflected downward by a greater amount, as is shown in figure 3.

Some points calculated from the results of Denison & Baum (1963) are also shown in figure 2. A comparison between these and the $M_1 = 0$ curve gives a good indication of the accuracy of the results presented herein. The small discrepancy occurring during the early stages of development is undoubtedly partly due to the small difference between the Blasius profile and its three-parameter (a_0, a_1 and a_2) approximation. However, the small size of Denison & Baum's original figure, and the necessity of transforming from semi-log co-ordinates to natural ones and back again, made precision impossible. Therefore the size of the discrepancy may well have been exaggerated. In any case, the fact that the exact asymptotic value of $\bar{u}_0$ according to Chapman (1949), namely 0·587, is attained in the $M_1 = 0$ case indicates very satisfactory accuracy for the later stages of development.

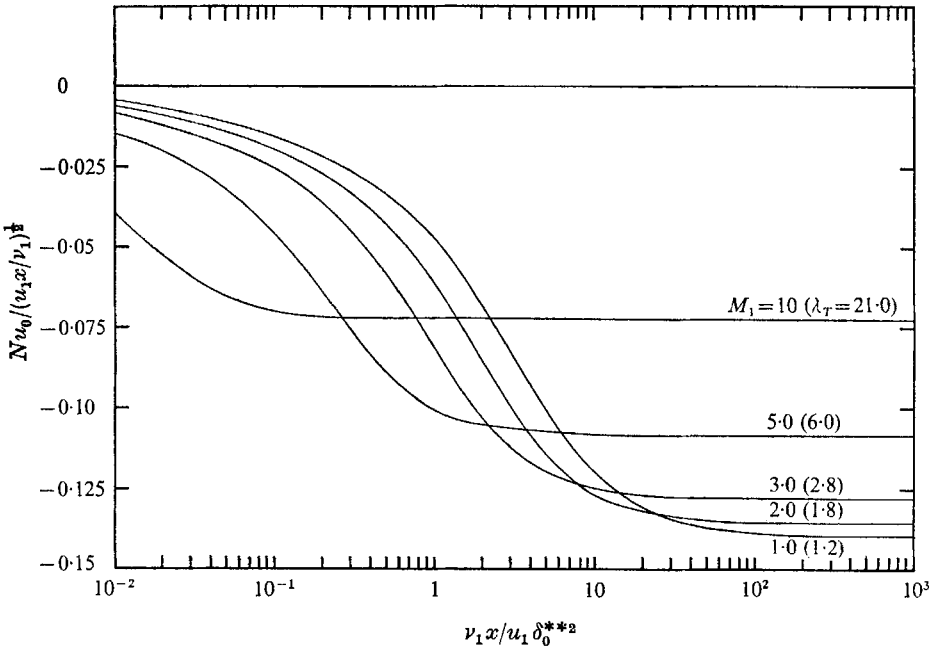

FIGURE 4. The effect of compressibility on the development of the local Nusselt number with the Blasius profile in $\bar{u}$, η co-ordinates used as an initial condition.

$$H_2/H_1 = H_W/H_1 = 1·0, \quad Pr = 0·72,$$

free-stream stagnation temperature = 275 °K, $\lambda_T = T_2/T_1$.

The effect of compressibility on the heat-transfer properties is illustrated in figure 4. The local Nusselt number at the dividing streamline is defined as

$$Nu_0 = +\frac{q_0 x}{k_1(T_1 - T_2)} = -\frac{k_0}{k_1}\frac{\partial T}{\partial y}\bigg|_0 \frac{x}{T_1 - T_2}.$$

Thus the heat transfer is positive when passing from the quiescent region to the main stream, in which case $T_1 < T_2$ and $Nu_0 < 0$.

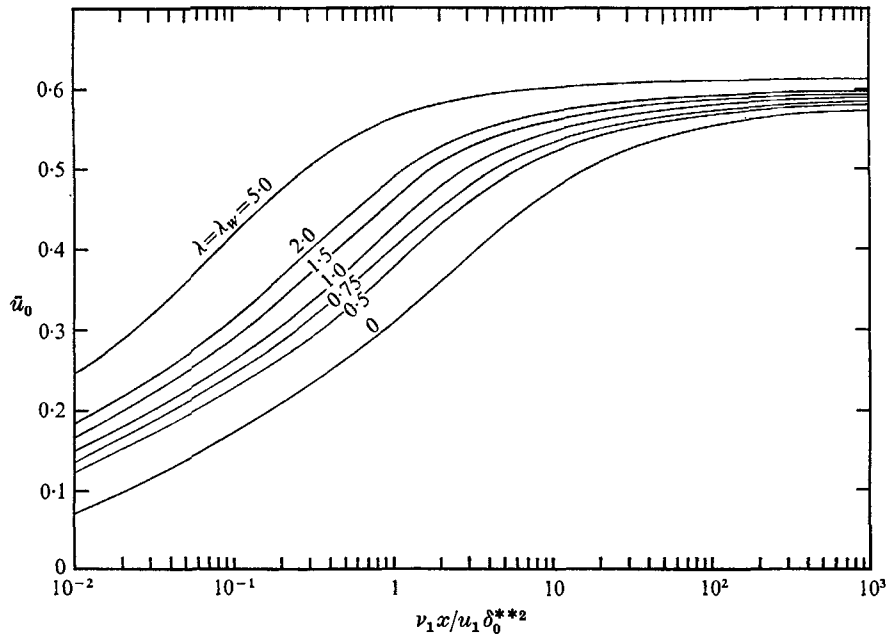

FIGURE 5. The effect of change in the total enthalpy ratio λ on the development of velocity at the dividing streamline with the Blasius profile in $\bar{u}$, η co-ordinates used as an initial condition. $M_1 = 3{\cdot}0$, $H_W/H_1 = H_2/H_1$, $Pr = 0{\cdot}72$, free-stream stagnation temperature = 275 °K.

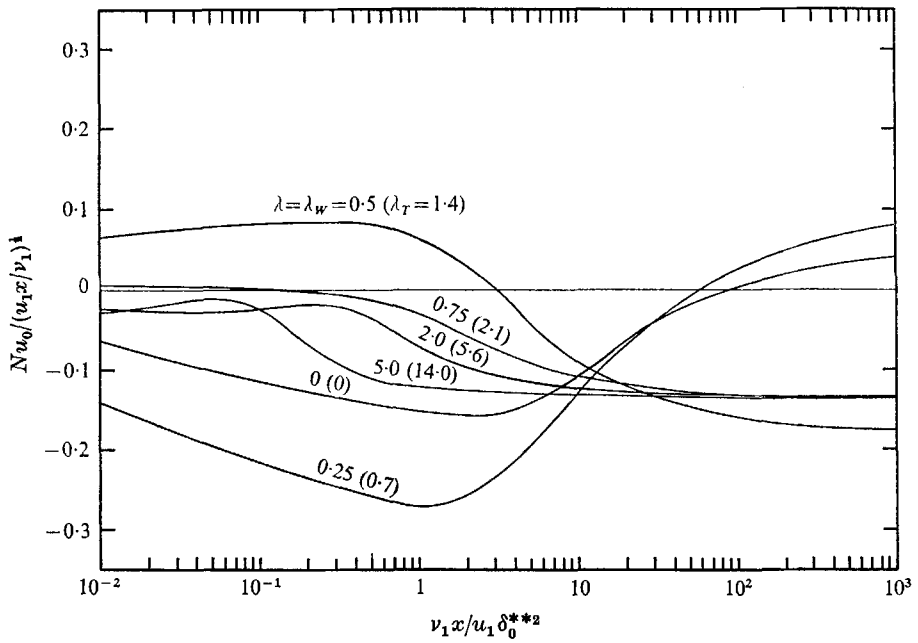

FIGURE 6. The effect of change in the total enthalpy ratio λ on the development of the local Nusselt number with the Blasius profile in $\bar{u}$, η co-ordinates used as an initial condition. $M_1 = 3{\cdot}0$, $H_W/H_1 = H_2/H_1$, $Pr = 0{\cdot}72$, free-stream stagnation temperature = 275 °K $\lambda_T = T_2/T_1$.

As might be expected, the greater temperatures associated with the higher Mach numbers are responsible for increased conduction rates, leading to a more rapid achievement of asymptotic conditions. Nevertheless, the final level for the heat-transfer coefficient steadily declines with an increase in Mach number. This is a direct consequence of viscous heating. Dissipation reaches its maximum at the point of peak shear stress, viz. the dividing streamline, bringing about a decrease in the effective temperature difference between this point and the main stream.

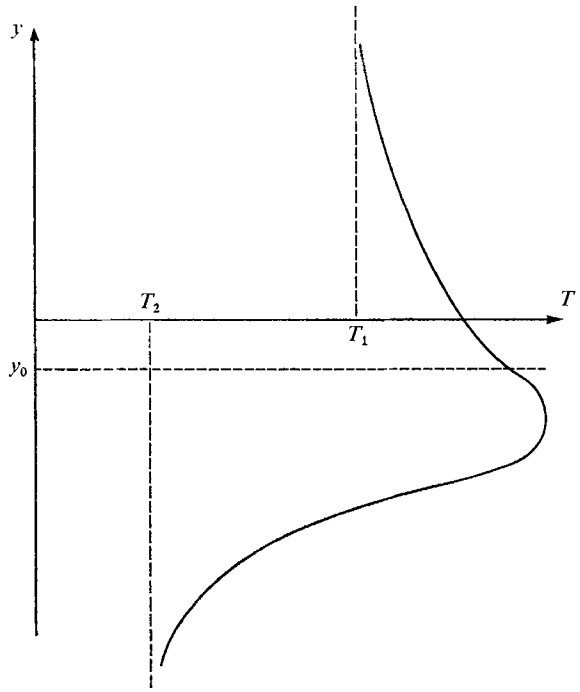

FIGURE 7. The general shape of the fully developed temperature profile for the case of $T_2/T_1 < 1$.

The effects of changing the total enthalpy ratio λ are illustrated in figures 5 and 6. The calculations were performed with $M_1 = 3{\cdot}0$. Since an increase in λ leads to higher dividing streamline temperatures, it is predictable that the diffusion rate will rise. This implies a more rapid growth to asymptotic conditions. Figure 5 confirms this prognostication. Once again the effects of viscous dissipation lead to the rather eccentric results corresponding to values of λ below 1·0 in figure 6. The temperature profiles corresponding to these curves have the general shape shown in figure 7 when fully developed.

The peak in the profile occurs because of viscous heating. In the early stages of development the locus of the points of maximum shear stress (where the effects of viscous dissipation are greatest) lies well above the dividing streamline. Consequently the temperature profile's peak is also located above y_0. In this way the initially negative Nusselt numbers for $\lambda = 0$ and 0·25 are explained.

However, as development progresses, the point of maximum shear stress moves towards the dividing streamline until the temperature gradient becomes negative at y_0.

The shear layer behaves very similarly when T_1' is slightly greater than one, e.g. see the curve in figure 6 corresponding to $\lambda = 0{\cdot}5$ (or $\lambda_T = 1{\cdot}4$). However, in this case since $T_1' - T_2$ is now positive the Nusselt number changes sign. When T_1' becomes greater than or equal to approximately $2{\cdot}5T_2$ the heat transfer at the dividing streamline is positive throughout development.

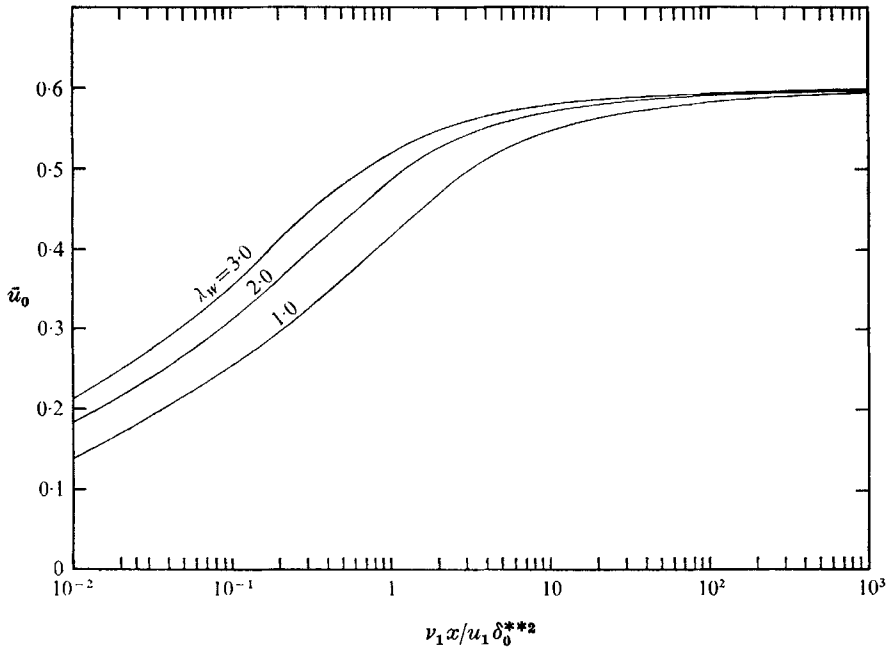

FIGURE 8. The effect of a discontinuity in the total enthalpy ratio at the origin on the development of velocity at the dividing streamline. $M_1 = 3{\cdot}0$, $H_2/H_1 = 2{\cdot}0$, $Pr = 0{\cdot}72$, free-stream stagnation temperature = 275 °K.

It is interesting to note that at a Mach number of 3·0, for which the calculations for figure 6 were performed, it is impossible to obtain negative heat transfer at the dividing streamline for a fully developed free shear layer. This means that the asymptotic level of the heat transfer is always such that heat flows towards the free stream at the dividing streamline. When λ exceeds 0·75 it appears from figure 6 that the asymptotic value of $Nu_0(u_1 x/\nu_1)^{\frac{1}{2}}$ becomes approximately invariant with λ having a value of about $-0{\cdot}135$. In addition, it could be remarked that figure 6 shows that for $\lambda < 0{\cdot}5$ (i.e. hot free stream) an estimate of heat transfer across the dividing streamline based on asymptotic conditions would probably be in serious error unless $\nu_1 x/u_1 \delta_0^{**2}$ exceeded 1000. However, in the case of $\lambda > 1{\cdot}0$, it is sufficient only that $\nu_1 x/u_1 \delta_0^{**2}$ be greater than 10.

Figure 8 shows the effect of a discontinuity in the total enthalpy ratio at the origin. The results are quite predictable although the magnitude of the effect is, perhaps, surprising.

The growth of $\bar{u}_0$ corresponding to three different initial velocity profiles is shown in figure 9. Falkner–Skan (1930) profiles were used, with the parameter, β, set at $-0{\cdot}18$, 0 and 1·0. Evans (1968) provided the data for the profiles which were assumed invariant with Mach number when cast in $\bar{u}, \eta$ co-ordinates. It can be seen that at $M_1 = 3{\cdot}0$ the influence of the shape of the initial profile is slight. However, the effect may be expected to be stronger at lower Mach numbers.

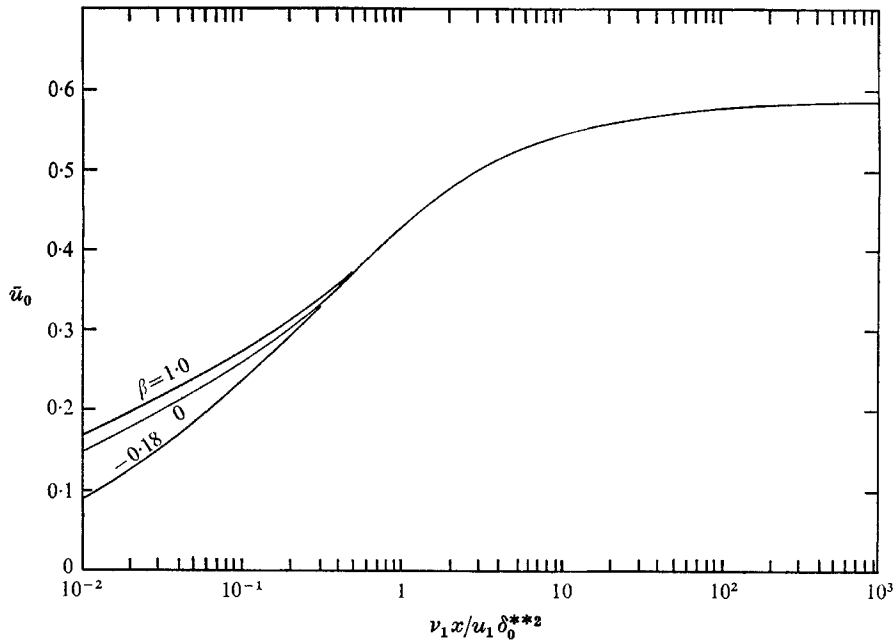

FIGURE 9. The development of velocity at the dividing streamline for different initial velocity profiles with the Falkner–Skan family of profiles in $\bar{u}$, η co-ordinates used as initial conditions. β is the Falkner–Skan parameter, $M_1 = 3{\cdot}0$, $H_2/H_1 = H_W/H_1 = 1{\cdot}0$, $Pr = 0{\cdot}72$, free-stream stagnation temperature 275 °K.

5. Conclusions

(i) The method of numerical integration presented could easily be modified for application to more involved problems, e.g. the case of $u_2 \neq 0$, and confined mixing.

(ii) The calculated results indicate that both compressibility and stagnation enthalpy difference have a great influence on the development of free shear layers.

(iii) The development is also strongly affected by a temperature discontinuity at the origin.

(iv) The influence of the form of initial velocity profile is only appreciable during the early stages of development.

(v) Calculations for the heat transfer across the dividing streamline, based on asymptotic conditions, are unlikely to be accurate unless $\nu_1 x/u_1 \delta_0^{**2}$ exceeds 1000 when H_2 is less than $0{\cdot}5H_1$.

The research leading to this paper was carried out at the Department of Aerospace Engineering, University of Cincinnati with the guidance of Dr Widen Tabakoff. It was supported by N.A.S.A. under Grant NGL 36-004-014.

REFERENCES

BATCHELOR, G. K. 1956 *J. Fluid Mech.* **1**, 388.

BROWN, W. B. & DONOUGHE, P. L. 1951 *N.A.C.A. Tech. Note*, 2479.

CARPENTER, P. W. 1970 Ph.D. dissertation, Department of Aero. Eng., University of Cincinnati.

CHAPMAN, D. R. 1949 *N.A.C.A. Rep.* no. 958.

CHAPMAN, D. R. 1950 *N.A.C.A. Rep.* no. 1051.

DENISON, M. R. & BAUM, E. 1963 *A.I.A.A. J.* **1**, 342.

DORODNITSYN, A. A. 1962 In *Advances in Aeronautical Sciences*, vol. 3. Pergamon.

EVANS, H. L. 1968 *Laminar Boundary-Layer Theory*. Addison-Wesley.

FALKNER, V. M. & SKAN, S. 1930 *Aero. Res. Counc. R. & M.* 1314.

GOLDSTEIN, S. 1930 *Proc. Camb. Phil. Soc.* **26**, 1.

KORST, H. H. 1956 *J. Appl. Mech.* **23**, 593.

LOCK, R. C. 1951 *Quart. J. Mech. Appl. Math.* **4**, 42.

TING, L. 1959 *J. Math. Phys.* **38**, 153.